Hexachloroplatinate-Initiated Synthesis of Polyaniline/Platinum Composite

John M. Kinyanjui, Rebekah Harris-Burr, Jeffery G. Wagner, Neloni R. Wijeratne, and David W. Hatchett*

Department of Chemistry, University of Nevada, Las Vegas, 4505 Maryland Parkway, Las Vegas, Nevada 89154-4003

Received June 14, 2004; Revised Manuscript Received September 2, 2004

ABSTRACT: The chemical synthesis of polyaniline (PANI) is explored using hexachloroplatinate, $PtCl_6^{2}$. These studies provide a simple method for the spontaneous oxidation of aniline by $PtCl_6^{2-}$ and simultaneous formation of gram quantities of PANI/Pt composite. The degree of Pt incorporation and subsequent encapsulation is based on a multistep reduction/oxidation process. The first step involves the reduction of $PtCl_6^{2-}$ to $PtCl_4^{2-}$ or Pt(0) and formation of the aniline radical cation in solution. The further reduction of $PtCl_4^{2-}$ to Pt(0) can also occur after aniline oligomers and polymer are formed in solution. The platinum colloids act as nucleation sites for the polymer forming the PANI/Pt composite, which precipitates from solution. Elemental analysis, XPS, and FTIR studies of the material indicate the properties of the polymer are consistent with the formation of a polymer salt containing metallic Pt. SEM images indicate that the Pt particles have maximum diameters on the order of 0.5−1 μm with some aggregation of clusters on the surface of the polymer. The formation of the PAN/Pt composite salt influences the electronic properties of PANI/Pt lowering the conductance by $\sim 10^7$ relative to PANI without Pt. The conductivity in solution is sufficient such that the representative acid doping and PANI/Pt electrochemistry is observed in HCl.

Introduction

The unique chemical and electronic properties of conductive polymers such as polyaniline (PANI) and polypyrrole (PPY) have contributed to the continued research of the materials. Detailed studies of conductive polymers have centered on the influence of the method of preparation,[1−4] doping,[5−8] influence of chemical constituents,[9,10] and morphology[11,12] on the physical and chemical properties of the materials. For example, acid doping and the oxidation state of PANI have been shown to dramatically influence the conductivity of the polymer.[13−15] The conductivity of PANI has been reported to increases 6-fold as a function of pH decrease from 6 to 0.[16] The range of conductance values for PANI doped with HCl has been reported to be between 2 and 10 S/cm for multiple trials using a standard synthetic procedure.[17] Optimization of synthetic conditions has shown that the highest conductivity is obtained in when the polymer contains a nitrogen/dopant ratio of 0.5 and equal numbers of oxidized and reduced units in the polymer.[18]

PANI is unique among conductive polymers in that it can undergo both proton and anion doping as a function of applied potential and changing oxidation state of the polymer. The uptake and expulsion of ionic species from PANI membranes is based on the need to maintain charge neutrality in the polymer membrane. Anion uptake can be in the form of the acid species in solution or other more novel metallic anions including $AuCl_4^-$, $PtCl_4^{2-}$, $PtCl_6^{2-}$, and $PdCl_6^{2-}$, to name a few. Although the uptake of metallic and acid anions is the same, the expulsion of metallic anions does not typically occur. The metal anions $AuCl_4^-$, $PtCl_4^{2-}$, $PtCl_6^{2-}$, and $PdCl_6^{2-}$ are often reduced at the point of contact between the metallic anion and polymer.[19] The uptake and reduction of Pt,[20] Au,[19] Ag,[21] and Pd[22] ions in PANI has been controlled previously using electrochemical methods. Well-known chemical interactions at metal interfaces such as the catalytic and sensing properties of PANI/metal composites containing Pt[23−27] and Pd[28] have been examined using PANI/metal composites produced using electrochemical methods. In each case the metal species imparted unique chemical characteristics not initially present in acid-doped PANI. We are particularly interested in the catalytic properties of PANI/Pt composites produced chemically rather than electrochemically. However, the optimization and determination of the catalytic properties of the PANI/Pt composite described here are beyond the scope of this paper and will be the subject of a separate study.

The difference between the electrochemical and chemical synthesis centers around the method of metal inclusion. The reduction of metal anions in preformed polymer membranes results in the conversion of benzenoid units to quinoid units, creating an electron-deficient polymer. The intrinsic charge balance associated with optimized electronic properties is lost despite the level of acid doping present. For example, the electrochemical uptake and reduction of $AuCl_4^-$ has been shown to reduce the conductivity by $\sim 10^7$ relative to the pristine polymer in the presence of 1 M acid.[29] Although the acid concentration is sufficiently high to protonate both imine and amine groups in the polymer,[7] the uptake of Au into polymer actually resulted in a polymer with a *higher* oxidation state and *reduced* proton doping. The reduced proton doping can be attributed to metallic Au blocking the imine nitrogen sites.[30] In contrast, chemical methods can be used to maintain the optimum oxidation state and doping levels in the polymer. The metal in the system serves a purpose also providing nucleation sites for the forming polymeric chains in solution.

* Corresponding author. E-mail dahatchet@ccmail.nevada.edu.

10.1021/ma0488313 CCC: $27.50
Published on Web 10/23/2004

Scheme 1

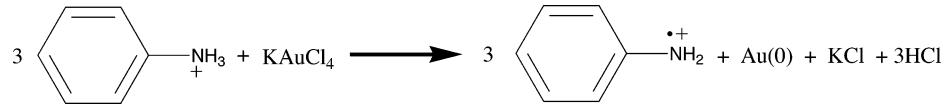

An alternative method for the synthesis of PANI/metal composites involves the use of metallic anions as the oxidant in the polymer initialization. Recently, chemical synthetic methods have recently been employed to produce gram quantities of PANI/Au composites with high conductivity.[30] In this study polymer initialization and growth was achieved using $AuCl_4^-$ as the chemical oxidant shown in Scheme 1. The PANI/Au composite produced chemically maintains its conductivity with equal number of oxidized and reduced units and high proton doping.

The chemical synthesis and characterization of PANI using oxidizing agents such as ammonium peroxydisulfate are well documented.[15,31,32] However, the direct chemical synthesis of polyaniline with metallic anions represents a new synthetic method for the formation of polymer/metal composites. The influence of the $PtCl_6^{2-}$ anion on the final oxidation state and the chemical composition of the composite must be examined. In addition, the final oxidation state of the metal and degree of Pt incorporation must be determined.

In this study we describe the direct synthesis of PANI/Pt composite using $PtCl_6^{2-}$ as the oxidizing agent in solutions containing acid (HBF_4). The synthetic process is detailed, and the chemical characteristics of system are evaluated and compared to PANI doped with HCl. In-situ UV/vis studies are used to monitor products and reactants simultaneously, and the polymer initialization reaction for the composite synthesis is proposed. In addition, SEM imaging is used to examine the polymer and Pt metal distribution and size. Elemental analysis, FTIR, and XPS studies are used to examine the chemical properties of the polymer with and without metal clusters. The conductance of dried PANI/HBF_4 and PANI/Pt is determined using a four-point resistance/conductance probe. The data suggest that the chemical and electronic properties of the polymer are directly influenced by the incorporation of Pt particles in PANI. Finally, the electrochemical doping of the PANI/Pt composite is performed to access the conductivity of the material in solution.

Experimental Section

Chemicals and Solutions. Tetrafluoroboric acid, HBF_4 (Aldrich, 44 wt %, 16872-11-0), HCl (Mallinckrodt, 36.5−38.0%, MFCD00011324), potassium hexachloroplatinate, K_2PtCl_6 (Alpha Aesar, 12169), potassium tetrachloroplatinate K_2PtCl_4 (Alpha Aesar, 11048), ammonium peroxydisulfate, $(NH_4)_2S_2O_8$, Mallinckrodt, 7277-54-0), *n*-phenyl-*p*-phenylenediamine (Alrich, 98%, 241393), and aniline, $C_6H_5NH_2$ (Aldrich, 99.9%, 13,293-4), were used as received. All solutions were prepared using 18.3 MΩ·cm water obtained from a Barnstead E-pure water filtration system.

PANI/Pt Composite Material Synthesis. Bulk PANI/Pt composite material used for FTIR and XPS measurements was produced by mixing 20 mL of 2.06×10^{-2} M K_2PtCl_6 with 20 mL of 0.22 M aniline both dissolved in 0.02 M HBF_4, representing a mole ratio of ∼1:10 (K_2PtCl_6 to aniline). The material was allowed to settle to the bottom of the reaction vessel prior to filtration. Once the product settled, it was collected using vacuum filtration, washed copiously with water, and dried under ambient conditions. Optical inspection shows no salt crystals formed on the surface from residual electrolyte. The filter paper used had pore diameters on the order of 3 μm. For comparison, the platinum particle size was on the order of 0.5−1 μm (verified by SEM). Therefore, any free platinum not encapsulated by the polymer could be washed through the filter paper during the extensive rinsing cycles. Samples were also dried in a vacuum oven at ∼70 °C prior to performing the FTIR experiments to remove residual water retained after air-drying. The synthetic process was repeated and resulted in an average product weight of 0.149 g ± 0.50% for the PANI/Pt composite. Pure PANI samples without platinum were obtained using previously published methods using ammonium peroxydisulfate as an oxidant in the presence of 1 M HBF_4.[13−16]

UV/Vis Spectroscopy. All spectra were obtained using a StellarNet EPP2000 fiber-optic spectrophotometer equipped with a D_2 lamp and tungsten filament source that were coupled into a single fiber. The transmitted light was collected after it passed through the cuvette by a second fiber and relayed to the detector. The integration time for the detector was typically 28 ms per scan for an average of 10 scans. The data acquisition times were varied to minimize the volume of data collected and stored. All UV/vis measurements were performed in a single, Teflon-capped, quartz cuvette with a path length of 1 cm. The in-situ characterization of reactants and products was performed using an episodic data capture routine. The data were collected at 15 min intervals. The in-situ UV/vis samples were prepared and monitored using 1.5 mL of 4.14×10^{-3} M K_2PtCl_6 and 1.5 mL of 0.05 M aniline in 0.02 M HBF_4, respectively. The overall concentration of each species in the cuvette was lowered to ensure optical transparency and the ability to obtain measurable signal throughout the reaction. The solution conditions employed were used to keep the magnitude of the signal below two absorbance units at all times.

FTIR Spectroscopy. All FTIR measurements were performed using a DIGILAB FTS-7000 spectrometer using a photoacoustic detector. Each sample was scanned 64 times with a resolution setting of 4 cm^{-1} and averaged to produce each spectrum. All samples were vacuum-dried overnight prior to measurement.

Scanning Electron Microscopy. SEM images of PANI/Pt composites were obtained using a JEOL 5600 electron microscope equipped with a backscattered electron (BSE) detector. The powder samples were ground to provide a uniform coating affixed to the sample holder using carbon tape. Measurements were performed at an acceleration voltage of 15 kV. Metal shadowing was not required prior to SEM measurement.

X-ray Photoelectron Spectroscopy. XPS data were collected using a Surface Science SSX-100 system with an Al Kα X-ray excitation source (1486.67 eV). The system was equipped with a hemispherical electron analyzer with a position-sensitive anode. The polyaniline/gold powder samples were mounted on a double-sided carbon tape placed on a piece of aluminum foil. For this study the carbon 1s peaks were assigned a binding energy of 284.6 eV and used as the energy reference. A chamber pressure of 5×10^{-9} Torr or lower was maintained for each sample measurements.

Conductance Measurements. A pellet of radius 1.25 cm was pressed from each material using 3 metric tons of pressure. The contacts were made using a Cascade Microtech C4S-64/50 probe head with tungsten carbide electrodes. The four-point probe sheet resistance of each pellet was then measured at locations across the surface of the pellet using an HP 34401A Digital multimeter connected through a Cascade Microtech CPS-05 probe station. Constant pressure for each measurement was maintained for the probed head contacting the substrate. A total of at least five measurements

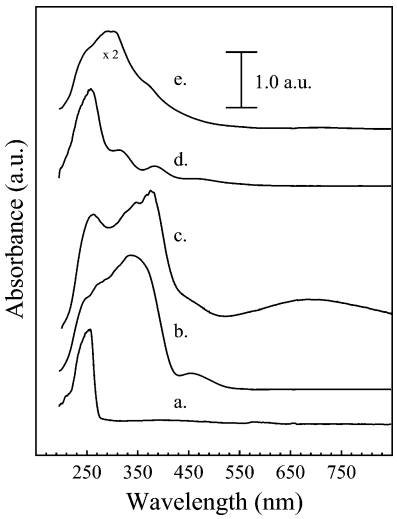

Figure 1. Bottom to top: UV/vis spectra of (a) 0.02 M aniline in 0.10 M HBF_4, (b) 4.14×10^{-3} M K_2PtCl_6, (c) chemically synthesized PANI/Pt colloid in aqueous solution obtained by mixing of 1.5 mL of 4.14×10^{-3} M K_2PtCl_6 and 1.5 mL of 0.05 M aniline in 0.02 M HBF_4 after 24 h, (d) 4.0×10^{-3} M K_2PtCl_4, and (e) filtrate solution after PANI/Pt precipitation and filtration.

at different location are presented with the corresponding relative standard deviations.

Electrochemical Apparatus and Conditions. All electrochemical measurements were performed using a CHI 660 potentiostat/galvanostat with included software. Unless noted, all solutions used were degassed with nitrogen, and a positive pressure was passed over the solution during all measurements. The experiments were performed in a one-compartment, three-electrode cell. All potentials are referenced to a Ag/AgCl electrode (3 M KCl filling solution). The counter electrode was a 0.5 mm platinum sheet with an area exceeding the immersed area of the working electrode by a factor of 2. The working electrode for Figure 6 was a glassy carbon electrode (Bioanalytical Systems, MF-2012 area = 7.07×10^{-2} cm^2) coated with a thin layer of paraffin oil. The PANI/Pt composite was affixed to the electrode by pressing the powder to the surface and tapping of the excess leaving a fine layer. This is a modified technique that has been used previously to examine the electrochemical properties of insoluble and ground samples.[33]

Results and Discussion

PANI/Pt Synthesis. The spectra of the reactants, reaction products, and the reaction filtrate are presented in Figure 1. The reactants aniline and $PtCl_6^{2-}$ are presented in parts a and b of Figure 1, respectively. Aniline has a single band at 254 nm, and $PtCl_6^{2-}$ has multiple bands which overlap with the aniline signal between 250 and 350 nm. In addition, one weak absorbance band for $PtCl_6^{2-}$ is resolved relative to aniline at 454.0 nm. This band for $PtCl_6^{2-}$ can be examined prior to and after completion of the reaction to determine whether the hexachloroplatinate anion has fully reacted. It is difficult to examine this band in situ to determine the concentration because there is significant overlap with absorbance bands associated with the polymer. For example, PANI has a $\pi-\pi^*$ transition between 320 and 360 nm and a polaron$-\pi$ transition at approximately 440 nm.[34−36] Shifts in the spectral bands are common for oligomers and polyaniline and indicate oxidative or morphological changes in the polymer.[37−40]

The spectrum of the reaction mixture containing 1.5 mL of 0.2 M aniline and 1.5 mL of 4.14×10^{-3} M K_2PtCl_6 in 0.20 M HBF_4 solution is presented in Figure 1c (t = 24 h). The emergence of the polymeric bands associated with the product can be observed as an increase in intensity of the absorbance band located at 381 nm. In addition, a broad, weak absorbance band at 689 nm emerges. The assignment of the band located at 381 nm is difficult because it lies between the $\pi-\pi^*$ transition of the benzene ring for the polymer and the band associated with the polaron$-\pi$ transition. In addition, convolution of the absorbance from the product and reactants makes it difficult to make an assignment. However, the band at 689 nm has been assigned previously to the localized polaron$-\pi$ transition of the polymer.[33−35]

The degree of overlap between the product and reactants absorbance bands minimizes the ability to evaluate concentrations of individual species (in situ) during the polymerization process. Therefore, the degree of $PtCl_6^{2-}$ reduction, formation of polymer, and residual oligomeric material in the system were examined after the reaction ceased using the filtrate (Figure 1e, the absorbance has been increased by a factor of 2 for clarity). The benefit of examining the filtrate is that the overlapping bands associated with the polymer are eliminated. In Figure 1e, the absence of an absorbance band at 454.0 nm marks the complete reduction of $PtCl_6^{2-}$. The broad absorbance with a small shoulder at 380.0 nm is *not* solely that of unreacted anilinium ion. Although $PtCl_4^{2-}$ is a possible candidate (Figure 1d), the absorbance of the filtrate between 270 and 330 nm is at much higher intensity. Only a weak band centered at 330 nm is present in UV/vis spectrum of $PtCl_4^{2-}$. The data does not preclude that there is a contribution from $PtCl_4^{2-}$. However, the formation of soluble, short-chain polymeric species likely contributes to the absorbance between 270 and 330 nm. Oligomeric species of different lengths can remain soluble in solution giving rise to the broad absorbance band encompassing the wavelength range in question.[41,42] It is likely that they provide the largest contribution to the absorbance in the spectral range in question.

In-Situ UV/vis Spectroscopy of PANI/Pt Composite Synthesis. The chemical reaction of a mixture of 1.5 mL of 4.14×10^{-3} M K_2PtCl_6 and 1.5 mL of 0.05 M aniline in 0.20 M HBF_4 was monitored for 48 h using in-situ UV/vis spectroscopy. A high mole ratio of ~1:12 K_2PtCl_6 to aniline was used to facilitate the complete reaction of $PtCl_6^{2-}$ in the solution. The mixed absorption bands of both aniline and $PtCl_6^{2-}$ are observed between 200 and 290 nm in Figure 2a. The emergence of the characteristic $\pi-\pi^*$ and polaron$-\pi$ bands associated with the polymer appear as increasing absorbance between 300 and 400 nm and 689.0 nm, respectively. In addition, a clear shift in baseline absorbance is observed indicative of light scattering effects due to Pt colloids formed in solution. The results indicate the reaction of $PtCl_6^{2-}$ with aniline and the formation of the polymer in solution are directly linked.

The first spectrum of the series (~1 h) was subtracted from each subsequent spectrum to highlight the emerging absorbance bands of the product during the reaction in Figure 2b. The characteristic polymeric bands emerge for the $\pi-\pi^*$ (320−400 nm) and polaron$-\pi$ (689 nm) transitions associated with the formation of the polymer. The increasing baseline absorbance is consistent with increased light scattering by Pt colloids formation in solution.

Scheme 2

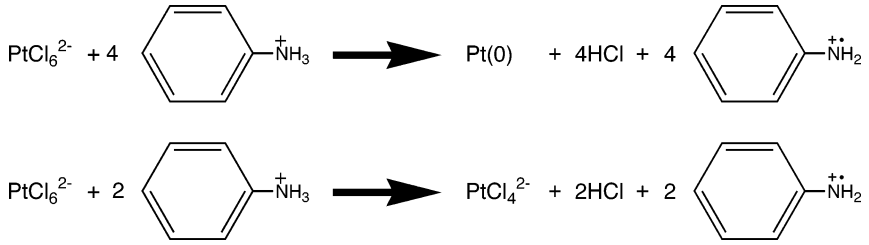

Scheme 3

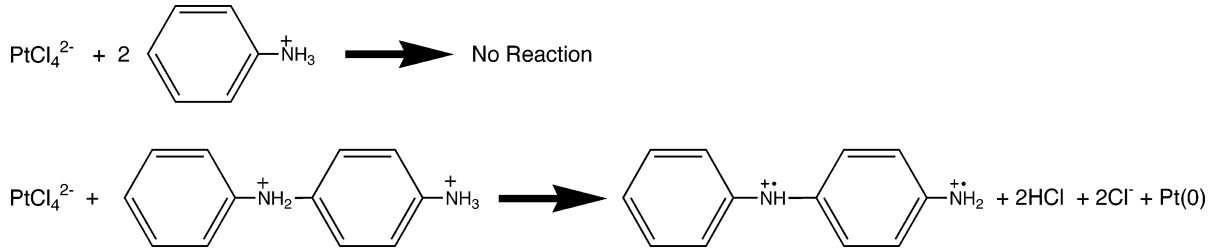

Scheme 4

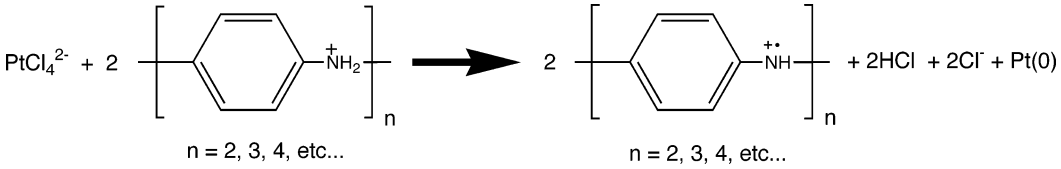

The absorbance over the course of the experiment is marked by the emergence of absorbance bands at 347, 382, and 689 nm (inset, Figure 2b). The band at 347

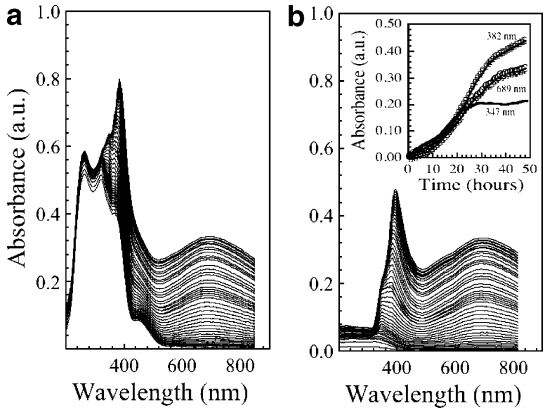

Figure 2. (a) In-situ UV/vis spectra of a mixture of 1.5 mL of 4.14×10^{-3} M K_2PtCl_6 and 1.5 mL of 0.05 M aniline in 0.02 M HBF_4. The data shown includes spectra obtained every hour for 48 h. (b) Emerging product bands after subtracting the first spectrum from all other spectra over the 48 h. Inset: plot of UV/vis absorbance intensity vs time for the product absorbances at 347, 382, and 689 nm.

nm emerges first and continues to increase in intensity over the first ~20 h. The absorbance intensity of this band becomes constant after 20 h, while the bands at 382 nm ($\pi-\pi^*$) and 689 nm (polaron$-\pi$) continue to increase in intensity. Genies and co-workers showed that absorbance bands for the polymer located below 400 nm can be attributed to the formation of soluble polymer intermediates and long chain PANI.[43] Wei and coworkers have observed this same trend while monitoring species present in the reaction mixture during the electrochemical formation of polyaniline.[44] These studies confirm the initial product formed in the synthesis of polyaniline is the oligomeric species followed over time by of variable chain length intermediates. The oligomeric building blocks form the long polymeric of the polymer, which precipitate when the solubility is exceeded (not shown).

Mechanism for the Formation of PANI/Pt Composites. The UV/vis absorbance at 347 nm can be used as an indicator in the synthetic process. The spontaneous reduction of $PtCl_6^{2-}$ forms the anilinium ion and initiates the formation of short chain oligomeric units in solution. Once the reduction of the $PtCl_6^{2-}$ ceases, the formation of the aniline radical cation ceases and the formation of intermediate structures slows. The synthetic process can be divided into two reduction steps on the basis of two possible reactions with $PtCl_6^2$. The polymer initialization can *only* occur through the reaction of $PtCl_6^{2-}$ with the anilinium cation to form the radical cation, $PtCl_4^{2-}$, and Pt(0) based on one of the reactions in Scheme 2.

Previous studies in our laboratory have shown that no reaction occurs between K_2PtCl_4 and the anilinium ion over a period of 1 month. In contrast, $PtCl_4^{2-}$ and the protonated dimer, *n*-phenyl-*p*-phenylenediamine, do react to form the PANI/Pt composite. The corresponding reactions are shown in Scheme 3. The FTIR spectra for the polymer metal composites produced using $PtCl_6^{2-}$/aniline and $PtCl_4^{2-}$/*p*-aminodiphenylamine were indistinguishable.

From these studies it can be concluded that the thermodynamic barrier associated with the oxidation of the short-chain oligomers is lower in comparison to the oxidation of the anilinium ion. Subsequently, $PtCl_4^{2-}$ can only react when short-chain oligomeric or polymeric species are present in solution. The spectroscopic data indicate that $PtCl_6^{2-}$ produces intermediate species in solution that are used as building blocks in the polymerization reaction (reaction shown in Scheme 4).

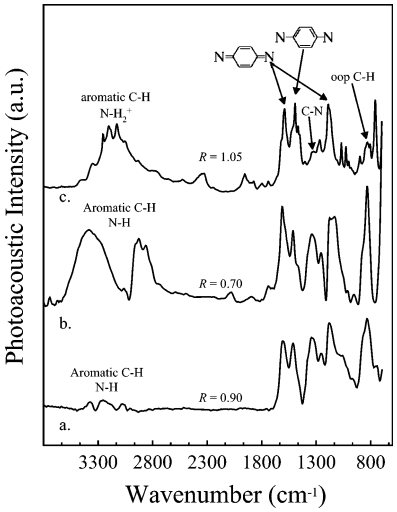

Figure 3. Photoacoustic FTIR spectra of (a) pure PANI/HBF_4 (without Pt particles), (b) pure PANI/HCl (without Pt particles), and (c) PANI/Pt composite produced during chemical synthesis using $PtCl_6^{2-}$ as the oxidant. FTIR band assignments and the ratio R, of the reduced and oxidized units, are labeled for clarity.

There is no direct spectroscopic evidence that all of the $PtCl_4^{2-}$ is fully reduced to Pt(0). However, it is assumed on the basis of the increasing baseline in Figure 2a,b that a large percentage of the Pt is metallic. The nucleation and growth of PANI at gold and platinum surfaces is well-known and an integral part of the electrochemical synthesis of the polymer membranes.[45−47] The synthesis with $PtCl_6^{2-}$ is clearly different because there is no bulk metal interface for nucleation. The nucleation and interaction of the polymer at colloidal Pt interfaces occurs as polymeric units are formed in solution simultaneously with the metal species. The nucleation and growth of the polymer onto colloidal Pt in the solution represents a significant deviation from previous mechanisms for the formation of PANI and PANI/metal composites using spontaneous nucleation or electrochemical reduction. The process is terminated by the precipitation of the material as the solubility of the forming PANI/Pt composite is exceeded.

Characterization of PANI/Pt Composite. FTIR Spectroscopy of PANI/Pt Composites. The IR spectroscopy of PANI/Pt and PANI/HBF_4 was examined to determine how the growth of the polymer and incorporation of Pt metal influence the chemical properties of the polymer. FTIR analysis of the fingerprint region between 700 and 1600 cm^{-1} is particularly useful for examining the resonance modes of the benzenoid and quinoid units and individual bonds (i.e., out-of-plane C−H and C−N) of PANI.[7] The FTIR spectra of pure PANI/HBF_4, PANI/HCl, and PANI/Pt are presented in Figure 3a−c. The characteristic ring bands for aromatic C−C stretching are located at 1597−1590 and 1512−1493 cm^{-1} for the pure polymer samples and the composite, respectively. In addition, the IR bands for the out-of-plane C−H can be compared with values between 832 and 825 cm^{-1} for the materials. These values are consistent with previously determined IR bands for PANI doped with a variety of different acids.[7]

The characteristic bands associated with the benzenoid phenyl ring (∼1500 cm^{-1}) and quinoid phenyl ring (∼1590 cm^{-1}) can also be used to estimate the oxidation state of the polymer. The ratio, R, of oxidized vs reduced units is obtained by integrating the corresponding IR bands. The most conductive form of PANI is the emeraldine salt where the benzenoid and quinoid units are approximately equal (i.e., $R = 1$). Integration of the peaks for PANI/HBF_4, PANI/HCl, and PANI/Pt gives values of $R = 0.90$, $R = 0.70$, and $R = 1.05$, respectively. This treatment makes no assumption concerning the proton or anion doping in the polymer. However, the values indicate that the PANI/HBF_4 and PANI/Pt materials have approximately equal numbers of oxidized and reduced units. The value for PANI/HBF_4 indicates that HCl directly influences the oxidation state of the polymer resulting in more oxidized units. The values for R can be obtained using the following diagram and equation:

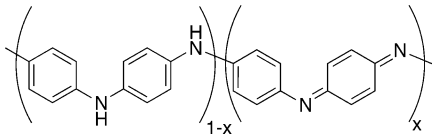

where

$$R = \frac{1-x}{x} = \frac{\text{area}_{\text{reduced}}}{\text{area}_{\text{oxidized}}} = \frac{\text{area}_{\nu(1590\ \text{cm}^{-1})}}{\text{area}_{\nu(1590\ \text{cm}^{-1})}}$$

A value of $R = 1.05$ for PANI/Pt suggests that reduction of $PtCl_6^{2-}$ and $PtCl_6^{2-}$ primarily occurs through the oxidation of the monomer and oligomers during the polymer formation. A greater percentage of quinoid units (higher degree of oxidation) in the polymer would be expected if the Pt species were reduced after the formation of the polymer. The conversion of benzenoid to quinoid units has been observed previously after the electrochemical reduction of $AuCl_4^-$ in a preexisting PANI membrane.[31,32]

Significant changes can be observed with respect to the nitrogen heteroatom when Pt is incorporated into the polymer. The C−N moiety plays an important role in the analysis of the composite. A more significant shift in energy is observed for the C−N stretch when comparing the PANI/Pt composite to either PANI/HBF_4 or PANI/HCl. The characteristic C−N band is located at 1334 cm^{-1} for PANI/HBF_4 and PANI/HCl, shifting to 1316 cm^{-1} for PANI/Pt. For secondary aromatic amine salts the band is typically between 1350 and 1280 cm^{-1}.[48] The 18 cm^{-1} shift to lower energy represents a difference in chemistry and electron density at the nitrogen heteroatom after Pt incorporation. In addition, the relative intensity of the C−N bond is drastically reduced in the case of the PANI/Pt composite. The diminished signal is consistent with segregation of the electron density of the lone pair electrons (lower resonance stabilization) at the nitrogen due to strong interactions between the heteroatom and Pt metal. This trend is repeated for the out-of-plane C−H stretch. Segregation of electron density can also occur through the protonation and formation of the salt at the nitrogen heteroatom. The increased segregation of electron density from both factors reduces ring resonance thus significantly reducing the IR intensity of secondary bonds such as C−H and N−H, relative to the ring.[48]

Spectroscopic evidence for the formation of amine and imine salt can be obtained from the characteristic bands for the N−H and C−H bands between 2600 and 3600 cm^{-1}. The assignment of the N−H stretch of PANI/HBF_4 and PANI HCl is straightforward with an IR band at 3373 cm^{-1} (Figure 3a,b). In the case of PANI/HCl a very

broad N−H band is observed, indicating that hydrogen bonding plays a role in the resonance of the NH groups. A similar band assignment at 3347 cm^{-1} can be made for the N−H stretch in the PANI/Pt (Figure 3c). However, this signal represents only a small fraction of the total signal for the N−H and C−H spectral region for PANI/Pt. The composite has the characteristic aromatic C−H bands superimposed on a rather broad band for the N−H group. Typically, amine salts have a broad absorbance band between 2700 and 3200 cm^{-1} that overlaps with the aromatic C−H stretch. The FTIR data for the PANI/Pt exhibit a broad band between the values of 2700−3200 cm^{-1}, in direct agreement with the literature.

Combination bands are also indicative of amine salts between 1700 and 2000 cm^{-1} with the band at 2000 cm^{-1} having the highest intensity.[48] Four combination bands are observed in Figure 3b for the PANI/Pt composite, with the most intense band at 1953 cm^{-1}. One could argue that these IR bands represent the ring overtones typically observed for substituted aromatic rings. If this were the case, we would also expect to see the bands for the pure polymer in the absence of Pt because the same polymeric structure exists (i.e., para substitution). However, we do not see the bands in PANI/HBF_4, indicating that Pt interaction and the formation of the amine salt in the PANI/Pt composite is the key to the emerging overtone bands. The FTIR results suggest that Pt incorporation directly influence the chemical properties of the nitrogen heteroatom, which does not occur with normal anionic dopants. Although the interaction between Pt and nitrogen groups in PANI causes chemical changes, it is still unknown whether the interactions are electrostatic, covalent, or a combination of both.

Elemental Analysis. The elemental analysis of pure PANI/HBF_4 and PANI/Pt (with HBF_4) was conducted to determine the chemical composition of the organic component in each sample. In addition, the Pt content was determined for the PANI/Pt sample. The unit formula for the emeraldine salt ($R = 1$) form of PANI is $C_6H_{4.5}N$, without assuming a contribution from hydrogen due to proton doping. Values greater than 4.5 for hydrogen can be attributed to a higher degree of proton doping or a more reduced polymer (i.e., $R > 1$). In addition, any proton doping in the polymer requires the uptake of anions to maintain charge neutrality in the system. Anion uptake can be in the form of Cl^- from the reduction of $PtCl_6^{2-}$ to $PtCl_4^{2-}$ or $PtCl_4^{2-}$ to Pt(0) or F^- from BF_4^- uptake. Elemental analysis does not rule out the incorporation of either $PtCl_6^{2-}$ or $PtCl_4^{2-}$ at this point. However, XPS analysis is used to provide metal speciation in the PANI/Pt composite.

The percentage of Pt in the composite can be estimated to be ∼36% relative to the organic component using the elemental analysis data and XPS data. This is based on a value the total weight percentage of the elements C, H, N, O, B, Cl, and F in the sample (64%). To estimate the total theoretical amount of Pt that can be incorporated into PANI, the amount of Pt remaining in solution was considered to be negligible. Using the theoretical gram weight of the Pt that was delivered to the solution in comparison to the gram weight of the collected composite, the maximum weight percent of Pt relative to the polymer was estimated at 40%. This weight percent represents the theoretical maximum that is higher than the estimate from elemental analysis. However, the agreement between the theoretical and experimental data suggests that the vast majority of $PtCl_6^{2-}$ and $PtCl_4^{2-}$ is converted to metallic Pt and incorporated into the polymer.

Table 1. (a) PANI/HBF_4 and (b) PANI/Pt Elemental Analysis (C, H, N, F, S, Cl, B, O) Normalized to $N = 1.0$

element	% comp	moles	mole ratio	analysis ratio
		(a) PANI/HBF_4		
C	61.14	5.09	6.10	$C_{6.1}H_{5.0}N_{1.0}F_{0.4}S_{0.2}B_{0.1}O_{0.7}$
H	4.68	4.16	4.98	
N	13.03	0.83	1.00	
F	7.28	0.34	0.41	
S	6.39	0.18	0.22	
Cl	0.00	0.00	0.00	
B	0.97	0.09	0.11	
O[a]	10.01	0.63	0.72	
		(b) PANI/Pt		
C	56.17	4.68	6.09	$C_{6.1}H_{6.2}N_{1.0}F_{0.0}Cl_{0.9}B_{0.0}O_{0.4}$
H	4.77	4.73	6.16	Pt composition
N	10.75	0.76	1.00	weight % = 36%
F	0.00	0.00	0.00	
S	0.00	0.00	0.00	
Cl	23.83	0.67	0.88	
B	0.00	0.00	0.00	
O[a]	4.46	0.27	0.36	

[a] Oxygen content is estimated using the O/N ratio from XPS data.

The unit formula consistent with the emeraldine form of polyaniline, $C_6H_{4.5}N$, is based on equal number of oxidized and reduced units in the polymer, excluding proton doping.[18] The hydrogen value of greater than 4.5 from the elemental analysis can be attributed to either the degree of proton doping or a more reduced polymer. In addition, any excess proton in the system requires the uptake of anions to maintain charge neutrality. Anion uptake can be in the form of common ions Cl^- from $PtCl_6^{2-}$ reduction or BF_4^-. In the case of the PANI/HBF_4 products from the reduction of peroxydisulfate can also contribute to the anion doping. The balance of the charge associated with the proton doping is achieved through the uptake of anions in the system.

Parts a and b of Table 1 show the elemental composition of PANI/HBF_4 and PANI/Pt, respectively. Elemental analysis of PANI/HBF_4 in Table 1a provides a unit formula for PANI synthesis using peroxydisulfate ($C_{6.10}H_{4.98}N_{1.00}B_{0.11}F_{0.41}S_{0.22}B_{0.11}O_{0.72}$). A value of ∼5.0 for the hydrogen indicates that the polymer is proton doped (0.5). The data also show that the polymer contains anions consistent with both the protic acid HBF_4 and the chemical oxidant $S_2O_8^{2-}$. The value obtained for F (0.41) must be divided by four to take into account the stoichiometry of the BF_4^- anion as an estimate of the charge (0.1). A significant amount of S was also found in the polymer (0.22), indicating that the reduced peroxydisulfate plays a role in the doping. For comparison, the concentration of HBF_4 is 1 M while the concentration of peroxydisulfate was 0.25 M. However, the reduction of one peroxydisulfate ion during the aniline oxidation results in the formation of two SO_4^{2-} anions in the solution (∼0.5 M), which can readily act as an anion dopant in the polymer.[45] On the basis of the 2-fold difference in concentration between the anions present in solution, the polymer shows moderately higher affinity for SO_4^{2-} in comparison to BF_4^-. The contribution from SO_4^{2-} in terms of the charge would be on the order of 0.44. The overall anion doping charge (0.10 BF_4^- and 0.44 SO_4^{2-}) of 0.54 is consistent with the degree of proton doping (0.5) for the system.

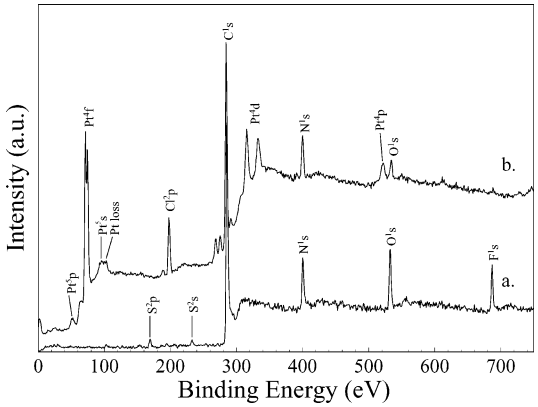

Figure 4. XPS surveys of (a) PANI/HBF_4 and (b) PANI/Pt composite. The XPS peaks are labeled for clarity.

The elemental analysis for PANI/Pt is significantly different than the results from PANI/HBF_4. Elemental analysis of the composite gives a unit cell of $C_{6.1}H_{6.2}N_{1.0}Cl_{0.9}O_{0.4}$. A significantly higher amount of hydrogen is present in the polymer composite in comparison to the pure material ($H_{6.2} - H_{4.5} = H_{1.7}$). The increase in hydrogen can be linked to a more reduced polymer ($R > 1$), which was confirmed in the FTIR analysis. It can also be indicative of a higher degree of proton doping. Elemental analysis shows no contribution from the acid anion BF_4^- (0.02 M). The only dopant observed in the elemental analysis of the PANI/Pt composite is the chloride ion from the reduction of 0.02 M $PtCl_6^{2-}$ in the form of Cl^- (0.9). The complete reduction of 0.02 M $PtCl_6^{2-}$ to Pt(0) would result in a Cl^- solution concentration of approximately 0.12 M. The lack of BF_4^- in the composite is likely due to the 6:1 concentration difference between Cl^- and BF_4^-.

$$\underset{0.02\ \mathrm{M}}{PtCl_6^{2-}} + 4e^- \rightarrow Pt(0) + \underset{0.12\ \mathrm{M}}{6Cl^-}$$

The combination increased hydrogen and chloride ion in the material indicates that the polymer contains a significant degree of protonated nitrogen groups in addition to more benzenoid units. The increase in chloride as a dopant is a direct result of increased protonation of the nitrogen groups within the polymer. These groups interact strongly with Cl^- through the formation of nitrogen/chloride salt groups. The elemental analysis and FTIR data both indicate that the PANI/Pt composite has functional groups consistent with the formation of a nitrogen/chloride salt.

X-ray Photoelectron Spectroscopy. Parts a and b of Figure 4 show the photoelectron spectra of PANI/HBF_4 and PANI/Pt, respectively. The presence of metallic Pt in the PANI/Pt spectrum is marked by the appearance of two Pt(0) peaks located at 71.2 and 74.5 eV, which can be assigned to Pt^4f. These values are consistent with the previously determined energies for metallic Pt.[49] The incorporation of Pt(II) and Pt(IV) is also possible. However, the characteristic ^4f XPS bands at 73.9 eV (Pt(II) ^4f) and 77.8 (Pt(IV) ^4f) are not observed in the XPS spectrum for the PANI/Pt.[49,50] The lack of XPS intensity at the energies associated with oxidized Pt indicates that the XPS signal is primarily due to metallic Pt in the polymer. Further support is provided by the appearance of XPS bands associated with metallic Pt (i.e., Pt^5p, Pt^5s, Pt_{loss}, Pt^4d, and Pt^4d) in Figure 4b.

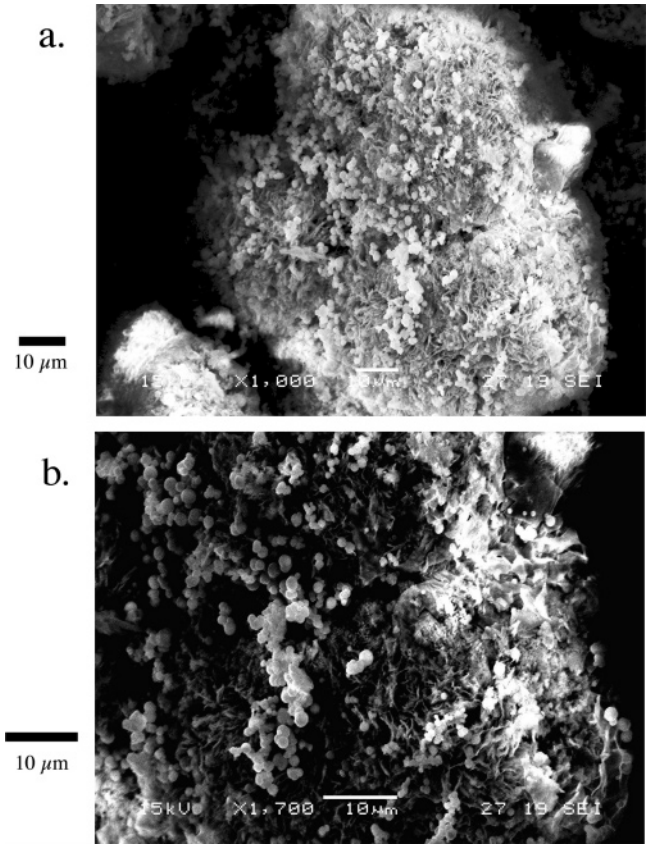

Figure 5. Transmission TEM diffraction image obtained from PANI/Pt composite: (a) 1000× magnification and (b) 1700× magnification. Scale bars are provided for clarity on the left of each figure.

Analysis of the dopant is based on the identification of dopant species F and Cl in each sample. The XPS band at 687 eV can be assigned to F, which is present only in PANI/HBF_4. Comparison of the N and F peaks allows the relative percent of dopant vs N in the unit formula to be compared to the XPS data for PANI/HBF_4. Each species must be first scaled by the element's XPS sensitivity factor ($F = 1$ and $N = 0.42$), and the stoichiometery of the doping species (four F per dopant anion) must be considered.

The XPS data confirm the degree of doping by BF_4^- with values of 0.09 for PANI/HBF_4. This number is consistent with the calculated value of 0.10 from elemental analysis. In addition, the low-energy sulfur peaks centered at 164 eV (S^2p) and 230 eV (S^2s) can be identified in Figure 4a, which are consistent with doping by the sulfate ion from the reduction of peroxydisulfate. The same treatment can be used to examine the Cl content in the PANI/Pt composite. The Cl^2p peak at 273 eV for Cl^- was integrated and scaled based on the relative sensitivity factor of 0.73. Comparison of the N and Cl XPS bands indicates that there are 0.95 Cl^- per nitrogen in the polymer metal composite. This value is slightly higher but agrees favorably with the value obtained from elemental analysis (0.90).

Scanning Electron Microscopy of PANI/Pt Composites. The XPS data provide evidence that metallic Pt is present in the polymer. SEM images are used to examine the platinum particles and polymer in Figure 5a,b. It must be stated that SEM is a surface technique that precludes the dispersion analysis of the metal into the polymer. However, incorporation of Pt within the polymer matrix is consistent with the known nucleation

properties.[45−47] The surface analysis of the composite provides the first visualization of the Pt particles with the polymer. The Pt particles appear on the surface as ∼1 μm spheres on the PANI surface in Figure 5a. The polymer appears a small ribbons of material interdispersed with the Pt particles. Some of the particles appear to be embedded in the polymer while others seem to be affixed to the surface.

A higher magnification SEM image of the same surface is presented in Figure 5b. The 0.5−1 μm particles can be seen nestled into the polymer and in the form of aggregates on the surface. The SEM data do not preclude that these particles are actually smaller with a PANI coating. However, the particles are absent when compared to chemically prepared PANI using peroxydisulfate and HBF_4 (not shown). Although the 3 μm porosity of the filter paper is sufficiently large to allow the 1 μm Pt particles to pass through during washing, the particles have remained contacted to the surface of the polymer. In addition, for the SEM measurements the composite was crushed into smaller particles. Despite these treatments, the PANI/Pt interaction is strong enough to minimize the loss of the metal during the collection and characterization of the composite.

Electronic Resistance/Conductance. From our elemental analysis data we find that PANI/HBF_4 is proton doped with $R = 0.90$, indicating that polymer contains relatively equal amounts of oxidized and reduced units. We also have sufficient proton doping in the material due to solution conditions employed during synthesis (1 M HBF_4). Proton doping and uptake of the counterion increase the number of free charge carriers in the polymer.[16] The PANI/Pt composite also contains a relative equal number of oxidized and reduced units, $R = 1.06$. However, the formation of an ionic amine/chloride salt and segregation of charge within the polymer decreases the amount of free charge carriers in the PANI/Pt composite. Therefore, we would expect the conductivity to be diminished relative to the acid-doped material.

The four-point probe sheet conductance for a pressed pellet of PANI/HBF_4 is 9.0 ± 10% S/cm. The sheet conductance of a pellet of PANI/Pt is $3.2 \times 10^{-7} \pm 10\%$ S/cm. The $\sim 10^7$-fold decrease in conductance indicates that Pt particle inclusion decreases the total number free of charge. Although both materials have a relatively equal number of oxidized and reduced units in the polymer, the electron density associated with the organic component is fixed after the insertion of Pt into the polymer. The reduction in free charge carriers for PANI/Pt results in large decreased in the conductance for the composite.

Electrochemistry of PANI/Pt Composites. The sheet conductivity measured for dry PANI/Pt falls well short of the conductivity measured for PANI doped with HCl, which is on the order of 2−10 S/cm.[17] As state previously, the two factors that influence the conductivity of the polymer are the oxidation state and degree of proton doping. A equal number of oxidized and reduced units with a proton doping level of 0.5 N/H is optimum, allowing the polymer to form resonance structures at the nitrogen atom which are essential in the flow of electron density through the polymer backbone.[18] If the vast majority of nitrogen sites are protonated and capped with a chloride ion, the ability to form the resonance structures is significantly diminished.[4,18]

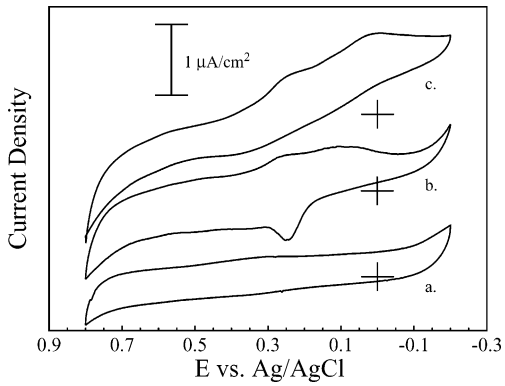

Figure 6. Cyclic voltammetric response of (a) glassy carbon electrode (GCE) in a nitrogen degassed 1 M HCl solution. (b) The same GCE electrode used in (a) coated with PANI/Pt in a nitrogen degassed 1 M HCl solution. (c) The same GCE used in (b) in a 1 M HCl solution *not* degassed with nitrogen.

However, proton doping is a parameter that can manipulated using electrochemical potential and solution conditions.[7] For example, the electrocatalytic properties of spontaneously formed PANI/Pt composite have been shown to be independent of the solution pH, indicating that the conductivity is actually enhanced by the incorporation of Pt.[51]

The electrochemical characteristics of PANI/Pt composite are examined in Figure 6. The background current for the glassy carbon electrode (GCE) in a degassed solution of 1 M HCl is presented in Figure 6a. The same GCE and solution are used to obtain the voltammetric response for the PANI/Pt composite in Figure 6b. The response for electrode coated with a thin layer of PANI/Pt composite shows the characteristic acid doping associated with the uptake and expulsion of proton from the polymer. The voltammetric response indicates that the conductivity in solution is sufficient to observe the oxidation/reduction characteristics of the material despite the low conductivity of the dry PANI/Pt composite. Finally, the GCE coated with PANI/Pt is examined in solution that are not degassed with nitrogen in Figure 6c. The reduction of oxygen can be examined in solutions that have not been degassed to determine whether the Pt in the composite acts as a potential-dependent catalyst. The voltammetric response in Figure 6c is characterized by an increased current density at 0.35 V vs Ag/AgCl relative to same electrode in degassed solutions of 1 M HCl. The voltammetric response is consistent with the reduction of dissolved O_2 by Pt in the composite, which indicates that potential dependent catalysis is possible with the chemically formed PANI/Pt composite.[23,52]

Conclusions

This study has shown that $PtCl_6^{2-}$ is a suitable oxidizing agent for the direct chemical polymerization of aniline. The formation of the PANI/Pt composite proceeds as $PtCl_6^{2-}$, $PtCl_4^{2-}$, aniline, and oligoaniline units react. Reduction of aniline ceases once the $PtCl_6^{2-}$ is consumed. The reaction of $PtCl_4^{2-}$ with oligomeric, short-chain units is energetically favorable and continues forming Pt(0) colloids. SEM and XPS data indicate that the Pt(0) particles (∼1 μm) strongly interact with the polymer. The synthesis provides a new method for producing gram quantities of polymer/metal composite materials with metal composition (up to ∼36 w/w%) and high chemical reproducibility. The results also indicate

that incorporation of Pt into PANI influences the electronic properties of the polymer through the formation of amine salt groups at the nitrogen heteroatoms. The conductance of the dry material is diminished by a factor of $\sim 10^7$ in comparison to dry PANI without Pt. The IR and elemental analysis suggest that the segregation of charge and formation of N/Cl ionic groups within the polymer is the key to the decrease in conductance of the dry composite. The electronic and chemical properties of the dry material do not prohibit the use of the material in solution where the conductivity is sufficiently high that the normal proton doping and catalytic reduction of oxygen can be observed for the polymer and Pt metal, respectively.

Acknowledgment. The authors acknowledge Dr. Allen Johnson for his help in obtaining the XPS results. The authors acknowledge J. Anthony Smith for his help in obtaining the conductance results. NSF EPSCoR of Nevada supported this research.

References and Notes

(1) Cairns, D. B.; Khan, M. A.; Perruchot, C.; Riede, A.; Armes, S. P. *Chem. Mater.* **2003**, *15*, 233.
(2) Zhou, M.; Pagels, M.; Geschke, B.; Heinze, J. *J. Phys. Chem. B* **2002**, *106*, 10065.
(3) Zeng, X.-R.; Ko, T.-M. *Polymer* **1998**, *39*, 1187.
(4) Huang, W.-S.; Humphrey, B. D.; MacDiarmid, A. G. *J. Chem. Soc., Faraday Trans. 1* **1986**, *82*, 2385.
(5) Salzer, C. A.; Elliott, C. M. *Chem. Mater.* **2000**, *12*, 2099.
(6) Lee, D.; Swager, T. M. *J. Am. Chem. Soc.* **2003**, *125*, 6870.
(7) Hatchett, D. W.; Josowicz, M.; Janata, J. *J. Phys. Chem. B* **1999**, *103*, 10992.
(8) Polk, B. J.; Potje-Kamloth, K.; Josowicz, M.; Janata, J. *J. Phys. Chem. B* **2002**, *106*, 11457.
(9) Henry, H. C.; Chen-Chan, J.; Timko, B. P.; Freund, M. S. *J. Electrochem. Soc.* **2001**, *148*, D155.
(10) MacDiarmid, A. G.; Epstein, A. J. *Synth. Met.* **1995**, *69*, 85.
(11) Demoustier-Champagne, S.; Stavaux, P.-Y. *Chem. Mater.* **1999**, *11*, 829.
(12) Sabatani, E.; Gafni, Y.; Rubinstein, I. *J. Phys. Chem.* **1995**, *99*, 12305.
(13) Jozefowicz, M. E.; Epstein, A. J.; Tang, X. *Synth. Met.* **1992**, *46*, 337.
(14) Joo, J.; Oh, E. J.; Min, G.; MacDiarmid, A. G.; Epstein, A. J. *Synth. Met.* **1995**, *69*, 251.
(15) Syed, A. A.; Dinesan, M. K. *Talanta* **1991**, *38*, 815.
(16) Travers, J. P.; Chroboczek, F.; Devereux, F.; Genoud, F.; Nechtschein, M.; Syed, A. A.; Genies, E. M.; Tsintavis, C. *Mol. Cryst. Liq. Cryst.* **1985**, *121*, 195.
(17) Stejskal, J.; Gilbert, R. G. *Pure Appl. Chem.* **2002**, *74*, 857.
(18) Ray, A.; Richter, A. F.; MacDiarmid, A. G.; Epstein, A. J. *Synth. Met.* **1989**, *29*, E151.
(19) Hatchett, D. W.; Josowicz, M.; Janata, J. *Chem. Mater.* **1999**, *11*, 2989.
(20) Kost, K. M.; Bartak, D. E. *Anal. Chem.* **1988**, *60*, 2379.
(21) Tian, Z. Q.; Lian, Y. Z.; Wang, J. Q.; Wang, S. J.; Li, W. H. *J. Electroanal. Chem.* **1991**, *308*, 357.
(22) Li, H.-S.; Josowicz, M.; Baer, D. R.; Engelhard, M. H.; Janata, J. *J. Electrochem. Soc.* **1995**, *142*, 798.
(23) Coutanceau, C.; Croissant, M. J.; Napporn, T.; Lamy, C. *Electrochim. Acta* **2000**, *46*, 579.
(24) Lai, E. K. W.; Bettie, P. D.; Holdcroft, S. *Synth. Met.* **1997**, *84*, 87.
(25) Ficicioglu, F.; Kadirgan, F. *J. Electroanal. Chem.* **1997**, *430*, 179.
(26) Kitani, A.; Akashi, T.; Sugimoto, K. *Synth. Met.* **2001**, *121*, 1301.
(27) Croisssant, M. J.; Napporn, T.; Leger, M. J.; Lamy, C. *Electrochim. Acta* **1998**, *43*, 2447.
(28) Drelinkiewicz, A.; Hasik, M.; Kloc, M. *Catal. Lett.* **2000**, *64*, 41.
(29) Kinyanjui, J. M.; Hanks, J.; Hatchett, D. W.; Smith, J. A.; Josowicz, M. *J. Electrochem. Soc.*, in press.
(30) Kinyanjui, J. M.; Hatchett, D. W.; Smith, J. A.; Josowicz, M. *Chem. Mater.* **2004**, *16*, 3390.
(31) Angelopoulos, M.; Asturias, G. E.; Ermer, S. P.; Ray, A.; Scherr, E. M.; Macdiarmid, A. G.; Akhtar, M.; Kiss, Z.; Epstein, A. J. *Mol. Cryst. Liq. Cryst.* **1988**, *160*, 151.
(32) Quillard, S.; Louarn, G.; Lefrant, S.; Macdiarmid, A. G. *Phys. Rev. B* **1994**, *50*, 12496.
(33) Almedia, C. M. V. B.; Geannetti, B. F. *Electrochem. Commun.* **2002**, *4*, 985.
(34) Higuchi, M.; Imoda, D.; Hiroa, T. *Macromolecules* **1996**, *29*, 8277.
(35) Venugopal, G.; Quan, X.; Johnson, G. E.; Houlihan, F. M.; Chin, E.; Nalamasu, O. *Chem. Mater.* **1995**, *7*, 271.
(36) Neoh, K. G.; Young, T. T.; Looi, N. T.; Kang, E. T.; Tan, K. L. *Chem. Mater.* **1997**, *9*, 2906.
(37) Han, C.-C.; Hong, S.-P. *Macromolecules* **2001**, *34*, 4937.
(38) Wang, P.; Tan, K. L.; Zhang, F.; Kang, E. T.; Neoh, K. G. *Chem. Mater.* **2001**, *13*, 581.
(39) Albuquerque, J. E.; Mattoso, L. H. C.; Balogh, D. T.; Faria, R. M.; Masters, J. G.; MacDiarmid, A. G. *Synth. Met.* **2000**, *113*, 19.
(40) Wei, Y.; Hsueh, K. F.; Jang, G.-W. *Macromolecules* **1994**, *27*, 518.
(41) Gruger, A.; El Khalki, A.; Colomban, P. *J. Raman Spectrosc.* **2003**, *34*, 438.
(42) Boyer, M. I.; Quillard, S.; Cochet, M.; Louarn, G.; Lefrant, S. *Electrochim. Acta* **1999**, *44*, 1981.
(43) Genies, E. M.; Boyle, A.; Lapkowski, M.; Tsintavis, C. *Synth. Met.* **1990**, *36*, 139.
(44) Wei, Y.; Tang, X.; Sun, Y. *J. Polym. Sci., Part A: Polym. Chem.* **1989**, *27*, 2385.
(45) Diaz, A. F.; Logan, J. A. *J. Electroanal. Chem.* **1980**, *111*, 111.
(46) Genies, E. M.; Tsintavis, C. *J. Electroanal. Chem.* **1985**, *195*, 109.
(47) Genies, E. M.; Syed, A. A.; Tsintavis, C. *Mol. Cryst. Liq. Cryst.* **1985**, *121*, 181.
(48) *Spectrometric Identification of Organic Compounds*, 5th ed.; Silverstein, R. M., Bassler, G. C., Morrill, T. C., Eds.; John Wiley and Sons: New York, 1991; pp 124−125.
(49) Liu, Z.; Lee, J. Y.; Han, M.; Chen, W.; Gan, L. M. *J. Mater. Chem.* **2002**, *12*, 2453.
(50) Atzei, D.; Filippo, D. D.; Rossi, A.; Porcelli, M. *Spectrochim. Acta A* **2001**, *12*, 1073.
(51) O'Mullan, A. P.; Dale, S. E.; Macpherson, J. V.; Unwin, P. R. *Chem. Commun.* **2004**, 1606.
(52) Lai, E. K. W.; Beattie, P. D.; Holdcroft, S. *Synth. Met.* **1997**, *84*, 87.

MA0488313